Large relativistic density pulses in electron-positron-ion plasmas

V. I. Berezhiani*
International Centre for Theoretical Physics, Trieste, Italy

S. M. Mahajan
Institute for Fusion Studies, The University of Texas at Austin, Austin, Texas 78712
and International Centre for Theoretical Physics, Trieste, Italy

(Received 2 March 1995)

The nonlinear propagation of circularly polarized electromagnetic waves with relativistically strong amplitudes in an unmagnetized hot electron-positron plasma with a small fraction of ions is investigated. The possibility of finding localized solutions in such a plasma is explored. It is shown that these plasmas support the propagation of "heavy bullets of light": nondiffracting and nondispersive electromagnetic pulses with large density bunching.

PACS number(s): 52.60.+h, 52.40.Db

I. INTRODUCTION

The nonlinear propagation of electromagnetic (e.m.) waves in electron-positron (*e-p*) plasmas is a subject of considerable interest [1]. Electron-positron pairs are thought to be a major constituent of the plasma emanating both from the pulsars and from the inner region of the accretion disks surrounding the central black holes in the active galactic nuclei [2]. The process of *e-p* pair creation occurs in relativistic plasma at high temperatures, i.e., when the plasma temperature exceeds twice the electron rest mass. In the standard cosmological model of the hot Universe (the Big Bang model), it is estimated that such temperatures ($T \sim 10^{10}$ K ~ 1 MeV) prevail up to times ~ 1 sec ($t \approx 1$ sec) after the Big Bang. In this epoch, the main constituents of the Universe are photons, neutrinos and antineutrinos, and *e-p* pairs [3]. As the plasma cools down, the annihilation process $e^+ + e^- \rightarrow \gamma + \gamma$ dominates and the e^+e^- pair concentration goes down according to the exponential law $n \approx \exp(-m_e c^2/T)$. Since the equilibration rates are fast in comparison with the changes in plasma parameters, an equilibrium *e-p* plasma should be present in the MeV epoch of the early Universe. Note that neutrinos and antineutrinos are in equilibrium with the primordial plasma only for $T > 3-5$ MeV ($t \leq 0.1$ sec) while at smaller temperatures their interactions can be neglected.

During the past few years, a considerable amount of work has been devoted to the analysis of nonlinear e.m. wave propagation in pure *e-p* plasmas. Although the *e-p* pairs form the dominant constituent of the aforementioned astrophysical and cosmic plasmas, a minority population of heavy ions is also likely to be present. For example, in the MeV epoch of the early Universe, the number of protons and neutrons is roughly $10^{-9}-10^{-10}$ (following from the present baryon asymmetry) of the number of light particles (electrons, neutrinos, and photons). Closer to the "beginning," at $t < 10^{-2}$ sec there were π mesons, K mesons, and proton-antiproton pairs as well as neutron-antineutron pairs in the primordial plasma. The minority ion population (even a very small fraction of the total) imparts interesting new properties to the composite system. Three-component plasmas have been studied, for example, in the context of pulsar magnetospheres [4]. In another study, theoretical investigations of relativistic collisionless shock waves in electron-positron-ion (*e-p-i*) plasmas of relevance to astrophysical sources of synchrotron radiation were carried out [5]. In our recent paper [6], we have shown that the present of even a small fraction of massive ions in the cold *e-p* plasma can lead to stable localized structures of relativistically strong e.m. radiation.

Would such structures survive if the plasma were relativistically hot? This question must be answered before one can explain their astrophysical as well as their cosmological consequences [7]. We must point out here that a stable, localized, e.m. solution with density excess may, coupled with gravity, create templates for confining matter and creating inhomogeneities necessary to understand the observed structure of the visible Universe.

In this paper we consider the propagation of relativistically strong e.m. radiation in a hot *e-p-i* unmagnetized plasma. We demonstrate that the presence of a minority ion species can indeed lead to the creation of stable, localized, nondispersive, and nondiffracting pulses that carry a large density excess within the region of field localization—the "heavy bullets of light."

II. BASIC EQUATIONS

Let us assume that the velocity distribution of the particles of species α is locally a relativistic Maxwellian. The dynamics of the fluid of species α, then, is contained in the equation [8]

*Permanent adress: Institute of Physics, The Georgian Academy of Science, Tbilisi 380077, The Republic of Georgia.

$$\frac{\partial}{\partial x_k}(U_\alpha^i U_{\alpha k} W_\alpha)-\frac{\partial}{\partial x_i}P_\alpha=\frac{1}{c}F^{ik}J_{\alpha k}\ , \tag{1}$$

where $U_\alpha^i\equiv[\gamma_\alpha,\gamma_\alpha \mathbf{u}_\alpha/c]$ is the hydrodynamic four-velocity, u_α is the hydrodynamic three-velocity of the fluid, $\gamma_\alpha=(1-u_\alpha^2/c^2)^{-1/2}$ is the relativistic factor, $J_{\alpha k}$ is the four-current, F^{ik} is the electromagnetic field tensor [9], and W_α is the enthalpy per unit volume

$$W_\alpha=\frac{n_\alpha}{\gamma_\alpha}m_{0\alpha}c^2 G_\alpha\left[\frac{m_{0\alpha}c^2}{T_\alpha}\right]\ . \tag{2}$$

Here $m_{0\alpha}$ and T_α are the particle invariant rest mass and temperature, respectively, n_α is the density in the laboratory frame of the fluid of species α, and $G_\alpha(z_\alpha)=K_3(z_\alpha)/K_2(z_\alpha)$, where $K_2(z_\alpha)$ and $K_3(z_\alpha)$ are, respectively, the MacDonald functions of the second and third orders ($z_\alpha=m_{0\alpha}c^2/T_\alpha$). The pressure $P_\alpha=n_\alpha^r T_\alpha$, where n_α^r is the density in the rest frame of fluid element of species α. Using the relation $n_\alpha^r=n_\alpha/\gamma_\alpha$, the relativistic particle pressure becomes

$$P_\alpha=\frac{n_\alpha}{\gamma_\alpha}T_\alpha\ . \tag{3}$$

Note that if our ultrarelativistic plasma is in full thermodynamic equilibrium with the photon gas (like in the early universe) one should also take into account the radiative pressure $P_R=\sigma T^4(\sigma=\pi/45h^3c^3)$ [3]. In this paper this effect, however, is neglected and will be discussed in a future publication.

The set of equations (1) can be rewritten (relativistic equation of motion)

$$\frac{d}{dt}(m_{0\alpha}G_\alpha\gamma_\alpha c^2)-\frac{1}{n_\alpha}\frac{\partial}{\partial t}P_\alpha=e_\alpha \mathbf{u}_\alpha\cdot\mathbf{E}\ , \tag{4}$$

$$\frac{d}{dt}(\mathbf{P}_\alpha G_\alpha)+\frac{1}{n_\alpha}\nabla P_\alpha=e_\alpha\mathbf{E}+\frac{e_\alpha}{c}(\mathbf{u}_\alpha\times\mathbf{B})\ , \tag{5}$$

where $\mathbf{P}_\alpha=\gamma_\alpha m_{0\alpha}\mathbf{u}_\alpha$ is the hydrodynamic momentum, $\mathbf{E}$ and $\mathbf{B}$ are the electric and magnetic fields, and $d_\alpha/dt=\partial/\partial t+\mathbf{u}_\alpha\cdot\nabla$ is the comoving derivative. Momentum equations similar to Eq. (5) have been widely used in literature (see references in Shukla *et al.* in [1]). In these papers, the thermal particle pressure P_α is taken to be $P_\alpha=n_\alpha T_\alpha$. The correct expression for P_α, however, must contain the relativistic factor γ_α [see Eq. (3)], which can be dropped only when the motion of the fluid elements is nonrelativistic (i.e., $p_\alpha^2/m_{0\alpha}^2c^2\ll 1$). Another important difference from the cold relativistic hydrodynamics is that the role of the particle mass is now played by the quantity $M_{\text{eff}}=m_{0\alpha}G_\alpha(z_\alpha)$, which depends on the temperature. For nonrelativistc temperatures ($T_\alpha\ll m_{0\alpha}c^2$, $z_\alpha\gg 1$), the effective mass reduces to $M_{\text{eff}}=m_{0\alpha}+5T_\alpha/2c^2$, while for the ultrarelativistic high temperatures ($T_\alpha\gg m_{0\alpha}c^2$, $z_\alpha\ll 1$), the effective mass becomes $M_{\text{eff}}=4T_\alpha/c^2\gg m_{0\alpha}$ [8]. For the ultrarelativistic case, the fluid inertia is primarily provided by the random thermal motion of the particles.

Taking the scalar product of Eq. (5) with $\mathbf{u}_\alpha$, subtracting the result from Eq. (4), and integrating the resulting relation, we find

$$\frac{n_\alpha z_\alpha}{\gamma_\alpha K_2(z_\alpha)}\exp[-z_\alpha G_\alpha(z_\alpha)]=\text{const.} \tag{6}$$

This is the adiabatic equation of state. In the nonrelativistic limit, Eq. (6) yields the usual result for a monoatomic ideal gas ($n_\alpha^r/T_\alpha^{3/2}=$const) and in the ultrarelativistic limit one obtains the equation of state for the photon gas ($n_\alpha^r/T_\alpha^3=$const).

To describe the e.m. wave propagation in a plasma we must couple the equations of motion with the Maxwell equations. In terms of the potentials defined by

$$\mathbf{E}=-\frac{1}{c}\frac{\partial\mathbf{A}}{\partial t}-\nabla\varphi\ ,\quad \mathbf{B}=\nabla\times A\ , \tag{7}$$

the field equations take the form (Coulomb gauge $\nabla\cdot A=0$)

$$\frac{\partial^2\mathbf{A}}{\partial t^2}-c^2\Delta\,\mathbf{A}+c\frac{\partial}{\partial t}(\nabla\varphi)-4\pi c\mathbf{J}=\mathbf{0} \tag{8}$$

and

$$\Delta\varphi=-4\pi\rho\ , \tag{9}$$

where

$$\rho=\sum_\alpha e_\alpha n_\alpha\ ,\quad \mathbf{J}=\sum_\alpha e_\alpha n_\alpha\mathbf{u}_\alpha \tag{10}$$

are, respectively, the charge and current densities. One now needs the continuity equation for the particle species α,

$$\frac{\partial n_\alpha}{\partial t}+\nabla\cdot(n_\alpha\mathbf{u}_\alpha)=0\ , \tag{11}$$

to close the system, which will now be studied to investigate the nonlinear propagation of relativistically intense e.m. wave in a relativistically hot three-component plasma made up of unmagnetized electrons, positrons, and massive ions; we aim at finding localized stable structures sustained by this plasma. The equilibrium state of the three-component system is characterized by an overall charge neutrality $n_0^-=n_0^++N_{0i}$, where n_0^-, n_0^+, and N_{0i} are the unperturbed number densities of the electrons, positrons, and ions, respectively. Because of their relatively large inertia, the ions do not respond to the dynamics under consideration and just provide a neutralizing background. The subscript α henceforth will indicate the electrons ($\alpha=-$) and the positrons ($\alpha=+$) only.

In terms of the dimensionless quantities

$$\begin{gathered}\mathbf{p}^\pm=\frac{\mathbf{p}^\pm}{m_e c}\ ,\quad n^\pm=\frac{n^\pm}{n_0^\pm}\ ,\quad T^\pm=\frac{T^\pm}{m_e c^2}\ ,\\ \mathbf{A}=\frac{|e|\,\mathbf{A}}{m_e c^2}\ ,\quad \phi=\frac{|e|\varphi}{m_e c^2}\ ,\quad \mathbf{r}=\frac{\omega_e}{c}\mathbf{r}\ ,\quad t=\omega_e t\ ,\end{gathered} \tag{12}$$

where $\omega_e=(4\pi n_0 e^2/m_e)^{1/2}$ is the electron Langmuir frequency, the entire set of defining equations reads

$$\frac{\partial^2\mathbf{A}}{\partial t^2}-\Delta\,\mathbf{A}+\frac{\partial}{\partial t}\nabla\phi+\left[\frac{n^-\mathbf{p}^-}{\gamma^-}-(1-\epsilon)\frac{n^+\mathbf{p}^+}{\gamma^+}\right]=0\ , \tag{13}$$

$$\Delta\phi = n^- - (1-\epsilon)n^+ - \epsilon \ , \tag{14}$$

$$\frac{d_\pm}{dt}[G(T^\pm)\gamma^\pm] - \frac{1}{n^\pm}\frac{\partial}{\partial t}\left[\frac{n^\pm T^\pm}{\gamma^\pm}\right] = \mp\left[\mathbf{u}^\pm \frac{\partial \mathbf{A}}{\partial t}\right] \mp (\mathbf{u}^\pm \nabla\phi) \ , \tag{15}$$

$$\frac{d_\pm}{dt}[G(T^\pm)\mathbf{p}^\pm] + \frac{1}{n^\pm}\nabla\left[\frac{n^\pm T^\pm}{\gamma^\pm}\right] = \mp\frac{\partial \mathbf{A}}{\partial t} \mp \nabla\phi \mp [\mathbf{u}^\pm \times (\nabla \times \mathbf{A})] \ , \tag{16}$$

$$\frac{\partial n^\pm}{\partial t} + \nabla\cdot(n^\pm \mathbf{u}^\pm) = 0 \ , \tag{17}$$

$$\frac{n^\pm}{\gamma^\pm T^\pm K_2\left[\frac{1}{T^\pm}\right]} \exp\left[-\frac{G^\pm}{T^\pm}\right] = \text{const} \ , \tag{18}$$

where

$$\gamma^\pm = [1+(\mathbf{p}^\pm)^2]^{1/2} \ , \quad \mathbf{u}^\pm = \frac{\mathbf{p}^\pm}{\gamma^\pm} \ , \tag{19}$$

and $d_\pm/dt = \partial/\partial t + \mathbf{u}^\pm\cdot\nabla$. The coefficient $\epsilon = N_{0i}/n_0^-$ is the ratio of the unperturbed ion to electron densities.

We begin this study by analyzing the one-dimensional propagation ($\partial/\partial z \neq 0$, $\partial/\partial x = 0 = \partial/\partial y$) of circularly polarized (CP) e.m. wave with a mean frequency ω_0 and a mean wave number k_0 along the z axis. The appropriate vector potential can be represented as

$$\mathbf{A}_\perp = \tfrac{1}{2}(\mathbf{x}+i\mathbf{y})A(z,t)\exp(ik_0 z - i\omega_0 t) + \text{c.c.} \ , \tag{20}$$

where $A(z,t)$ is a slowly varying function of z and t and $\mathbf{x}$ and $\mathbf{y}$ are the standard unit vectors. (The gauge condition allows us to adopt $A_z = 0$.) Writing the last term on the right-hand side of Eq. (16) as

$$\mathbf{u}^\pm \times (\nabla \times \mathbf{A}_\perp) = -u_z^\pm \frac{\partial \mathbf{A}_\perp}{\partial z} + \mathbf{z}\left[\mathbf{u}_\perp^\pm \cdot \frac{\partial \mathbf{A}_\perp}{\partial z}\right] \ , \tag{21}$$

the transverse component of the equation of motion (16) is immediately integrated to give

$$\mathbf{p}_\perp^\pm G^\pm = \mp \mathbf{A}_\perp \ , \tag{22}$$

where the constant of integration is set equal to zero since the particle hydrodynamic momenta are assumed to be zero at infinity where the field vanishes. The longitudinal motion of the plasma is determined entirely by the set consisting of the z component of the equation of motion (16),

$$\left[\frac{\partial}{\partial t} + u_z^\pm \frac{\partial}{\partial z}\right] G^\pm p_z^\pm + \frac{1}{n^\pm}\frac{\partial}{\partial z}\left[\frac{n^\pm T^\pm}{\gamma^\pm}\right] = \mp\frac{\partial\phi}{\partial z} \mp \left[\mathbf{u}_\perp^\pm \frac{\partial \mathbf{A}_\perp}{\partial z}\right] \ , \tag{23}$$

the "energy" conservation equation (15),

$$\left[\frac{\partial}{\partial t} + u_z^\pm \frac{\partial}{\partial z}\right] G^\pm \gamma^\pm - \frac{1}{n^\pm}\frac{\partial}{\partial t}\left[\frac{n^\pm T^\pm}{\gamma^\pm}\right] = \mp\left[\mathbf{u}_\perp^\pm \cdot \frac{\partial \mathbf{A}_\perp}{\partial t}\right] \mp \left[u_z^\pm \frac{\partial\phi}{\partial z}\right] \ , \tag{24}$$

and the continuity equation (17),

$$\frac{\partial n^\pm}{\partial t} + \frac{\partial}{\partial z}\left[\frac{n^\pm p^\pm}{\gamma^\pm}\right] = 0 \ . \tag{25}$$

Because of circular polarization of the e.m. wave $\gamma^\pm$ does not depend on the "fast" time (ω_0^{-1}) and [using Eq. (22)] can be written as

$$\gamma^\pm = \left[1 + \frac{|A|^2}{(G^\pm)^2} + (p_z^\pm)^2\right]^{1/2} \ . \tag{26}$$

Note that every quantity in Eqs. (23)–(25) varies on the slow time scale. It is now convenient to introduce new variables $\xi = z - v_g t$ and $\tau = t$, where $v_g = k_0/\omega_0$ is the group velocity of the e.m. wave packet. Assuming that $v_g \partial/\partial\xi \gg \partial/\partial\tau$ and integrating Eqs. (23) and (24), we get the integral of motion

$$G^\pm\left[1 + \frac{|A|^2}{(G^\pm)^2} + (p_z^\pm)^2\right]^{1/2} - v_g G^\pm p_z^\pm \pm \phi = \text{const} \ . \tag{27}$$

The constant of integration is determined by using the natural boundary condition that at infinity, the e.m. fields and the plasma momentum vanish. We also assume that $T_0^- = T_0^+ = T_0$, where T_0^- and T_0^+ are the equilibrium temperatures of electrons and positrons. Thus the constant of integration is found to be $G_0(T_0)$.

In this paper we consider the case of a transparent plasma ($\omega_0 \gg 1$) for which $v_g \approx 1$. After simple algebra, Eq. (27) yields

$$p_z^\pm = \frac{G^\pm}{2G_0}\left[1 + \frac{|A|^2}{(G^\pm)^2} - \frac{G_0^2}{(G^\pm)^2}\left[1 \mp \frac{\phi}{G_0}\right]^2\right] \times \left[1 \mp \frac{\phi}{G_0}\right]^{-1} \tag{28}$$

and

$$\gamma^\pm = \frac{G^\pm}{2G_0}\left[1 + \frac{|A|^2}{(G^\pm)^2} + \frac{G_0^2}{(G^\pm)^2}\left[1 \mp \frac{\phi}{G_0}\right]^2\right] \times \left[1 \mp \frac{\phi}{G_0}\right]^{-1} \ . \tag{29}$$

Integrating the continuity equation (25) we get

$$n^\pm = \frac{\gamma^\pm}{\gamma^\pm - p_z^\pm} \ . \tag{30}$$

From Eqs. (28)–(30) we derive important relations

$$\frac{n^\pm}{\gamma^\pm} = \frac{G^\pm}{G_0}\left[1 \mp \frac{\phi}{G_0}\right]^{-1} \ , \tag{31}$$

$$r^\pm - p_z^\pm = \frac{G_0}{G^\pm}\left[1 \mp \frac{\phi}{G_0}\right] \ , \tag{32}$$

which allow us to write the electron and positron densities fully in terms of the potentials ϕ and A (and the relativistic G factors)

$$n^{\pm}=\frac{(G^{\pm})^2}{2G_0^2}\left[1+\frac{|A|^2}{(G^{\pm})^2}\right]\left[1\mp\frac{\phi}{G_0}\right]^{-2}+\frac{1}{2}\ . \tag{33}$$

These expressions, along with Eqs. (20) and (22), help us to convert the Maxwell equations (13) and (14) into a set of coupled equations in φ and A,

$$2i\omega_0\frac{\partial A}{\partial\tau}+\frac{(2-\epsilon)}{\omega_0^2 G_0}\frac{\partial^2 A}{\partial\xi^2}+AG_0^{-1}\frac{\phi G_0^{-1}}{(1-\phi^2 G_0^{-2})}[\epsilon-(2-\epsilon)\phi G_0^{-1}]=0\ , \tag{34}$$

$$\frac{\partial^2\phi}{\partial\xi^2}=\frac{1}{2}\left[\frac{G^-}{G_0}\frac{[1+|A|^2(G^-)^{-2}]}{(1+\phi G_0^{-1})^2}-(1-\epsilon)\frac{G^+}{G_0}\frac{[1+|A|^2(G^+)^{-2}]}{(1-\phi G_0^{-1})^2}-\epsilon\right]\ , \tag{35}$$

where the wave frequency ω_0 satisfies the dispersion relation $\omega_0^2=k_0^2+(2-\epsilon)G_0^{-1}$, implying $v_g\approx 1$ for a transparent plasma for which $\omega_0\gg G_0^{-1/2}(1+|A|^2G_0^{-2})^{1/2}$ (placing an upper limit on the allowed wave amplitude) has been assumed. Equations (18), (34), and (35) constitute a closed set describing the nonlinear propagation of powerful CP e.m. waves of arbitrary (as long as $|A|<\omega_0$) amplitude in an unmagnetized, transparent hot electron-positron-ion plasma. For the case of a pure electron-positron plasma ($\epsilon=0$), we can see from Eq. (35) that the only solution consistent with the boundary condition $\phi(\infty)=0$ is $\phi=0$ everywhere (see also Refs. [10,11]). Comparing Eqs. (18) and (31) we find that the temperatures of the electron and positron fluids remain unchanged $T^-=T^+=T_0$. The potential vanishes because the equal effective masses of the electron and the positron fluids lead to equal radiative pressures. Equation (34), then, does not have a soliton solution; the CP e.m. waves cannot be localized in a pure electron-positron plasma.

Let us now introduce some heavy ions, i.e., a small but nonzero ϵ. The presence of even a small fraction of ions leads to "symmetry breaking" between electrons and positrons and consequently we can have a finite $\phi/G_0(\sim\epsilon)$. For $\phi/G_0\ll 1$ the temperature variation is also small $\Delta T^{\pm}/T_0\ll 1$, allowing us to write $G^{\pm}=G_0+G_0'\Delta T^{\pm}$, where $G_0'=dG_0/dT_0$. In this ordering, Eq. (31) becomes

$$\frac{n^{\pm}}{\gamma^{\pm}}=1+\frac{G_0'}{G_0}\Delta T^{\pm}\pm\frac{\phi}{G_0}\ , \tag{36}$$

while the "adiabatic" equation (18) reduces to

$$\frac{n^{\pm}}{\gamma^{\pm}}=1+\frac{G_0'-1}{T_0}\Delta T^{\pm}\ . \tag{37}$$

From Eqs. (36) and (37), it is easy to see that $\Delta T=\Delta T^-=-\Delta T^+$ and

$$\Delta T=\frac{\phi}{G_0}\left[\frac{G_0'}{G_0}-\frac{G_0'-1}{T_0}\right]^{-1}\ , \tag{38}$$

explicitly showing that, in the absence of charge separation ($\phi\to 0$), the temperature variation of the plasma vanishes ($\Delta T\to 0$).

To make further progress, let us assume that the characteristic length (L) of the wave satisfies the condition $L\gg(1+|A|^2G_0^{-2})^{-1/2}$. The assumption implies a major simplification; Eq. (35) can now be algebraically solved for φ,

$$\frac{\phi}{G_0}=\frac{\epsilon}{4}\frac{|A|^2}{G_0^2}\left[1+\beta+(1-\beta)\frac{|A|^2}{G_0^2}\right]^{-1}\ , \tag{39}$$

where the parameter

$$\beta=\frac{1}{2}\left[\frac{(G_0'-1)G_0}{T_0G_0'}-1\right]^{-1}\geq 0 \tag{40}$$

measures the relativistic temperature effects. In the cold plasma limit ($T_0\to 0$) $\beta\to 0$ and in the case of ultrarelativistic temperature ($T_0\to\infty$) β monotonically attains its asymptotic value $\beta=0.25$. Without loss of generality, we neglect β in Eq. (39). From (39), it follows that $\phi>0$; thus in the region of field localization, the electron temperature decreases and the positron temperature increases. If we now redefine the electron rest mass in Eq. (12) as $m_e\to m_eG_0(T_0)$, G_0 will disappear from Eqs. (34) and (39). Substituting (39) into (34) and neglecting ϕ^3 and higher orders, we obtain

$$2i\omega_0\frac{\partial A}{\partial\tau}+\frac{2}{\omega_0^2}\frac{\partial^2 A}{\partial\xi^2}+\frac{\epsilon^2}{8}f(|A|^2)A=0\ , \tag{41}$$

where

$$f(|A|^2)=1-\frac{1}{(1+|A|^2)^2}\ . \tag{42}$$

Thus the nonlinear propagation of CP e.m. waves in a hot electron-positron plasma with a small fraction of ions is described by the nonlinear Schrödinger equation (NSE) with a saturating nonlinearity, which comes naturally from our model. An equation of the exact same form as Eq. (41) was derived in our paper [6] for the cold plasma limit. The only difference is that now the rest mass of the charge particles has been replaced by a temperature-dependent effective mass. The temperature variation of the plasma does not play an important role during wave propagation. This is true even if we considered an isothermal equation of state. Note that these statements are valid for a transparent plasma when the group velocity of the e.m. pulses is close to velocity of light ($v_g\approx 1$).

We now generalize our results by allowing a transverse variation of the fields. If we assume that A depends weakly on the transverse coordinates [$A=A(\xi,x,y,\tau)$], i.e., $\partial A/\partial\xi\gg\nabla_\perp A$, Eq. (41) acquires an additional term $\Delta_\perp A$ [for a proper derivation, see (11)] and changes to

$$2i\omega_0\frac{\partial A}{\partial\tau}+\frac{2}{\omega_0^2}\frac{\partial^2 A}{\partial\xi^2}+\Delta_\perp A+\frac{\epsilon^2}{8}f(|A|^2)A=0\ . \tag{43}$$

In spite of the fact $\partial A/\partial\xi\gg\nabla_\perp A$, the second and the third terms may have comparable magnitudes because of the transparency of the plasma ($\omega_0\gg 1$). In the following

sections we investigate the solutions of (43), which after the self-evident renormalization of the variables can be presented as

$$i\frac{\partial A}{\partial \tau}+\frac{\partial^2 A}{\partial \xi^2}+\Delta_\perp A+\left[1-\frac{1}{(1+|A|^2)^2}\right]A=0\ . \tag{44}$$

III. STATIONARY PROPAGATION

In this section we seek the localized soliton solutions of (44) under a variety of conditions. Let us start with deriving one-dimensional structures by dropping the transverse derivative term. For the stationary solitons, the ansatz (Ω is a constant corresponding to a nonlinear frequency shift)

$$A=A(\xi)\exp(i\Omega^2\tau) \tag{45}$$

reduces Eq. (44) to

$$\frac{d^2A}{d\xi^2}-\Omega^2 A+A\left[1-\frac{1}{(1+A^2)^2}\right]=0\ . \tag{46}$$

Invoking the boundary conditions appropriate to a localized solution, i.e., $A=0=dA/d\xi$ as $|\xi|\to\infty$, Eq. (46) can be readily integrated and allows solitonlike solutions for $\Omega^2<1$. There are several ways in which the exact implicit solution of Eq. (46) can be displayed. The most revealing perhaps is the form

$$|\xi|=\frac{\cos^{-1}[(1-\Omega^2)(1+A^2)]^{1/2}}{(1-\Omega^2)^{1/2}}+\frac{1}{2\Omega}\ln\frac{\Omega(1+A^2)^{1/2}+[1-(1-\Omega^2)(1+A^2)]^{1/2}}{\Omega(1+A^2)^{1/2}-[1-(1-\Omega^2)(1+A^2)]^{1/2}}\ . \tag{47}$$

For all values of Ω^2, Eq. (47) can be satisfied at $|\xi|=0$ if $(1-\Omega^2)[1+A(0)^2]=1$, leading to $A(0)^2\equiv A_m^2=\Omega^2/(1-\Omega^2)$, where the amplitude A_m is the maximum value A can attain. Clearly $A_m\to 0$ as $\Omega\to 0$ and A_m becomes large as $\Omega\to 1$. Remembering that A is exactly equal to the particle hydrodynamic momentum measured in $M_{\text{eff}}c$, large A_m corresponds to a highly relativistic plasma, the principal regime of interest for this paper.

Let us begin the analysis of Eq. (47) by determining the asymptotic behavior of A. As long as Ω is not extremely close to unity, it is only the second term that can provide the balance as $|\xi|\to\infty$. Thus, for sufficiently large $|\xi|$, Eq. (47) leads to the exponentially decaying solution (for all Ω)

$$A_{\text{asy}}\simeq\Omega\,\text{sech}\Omega|\xi|\ . \tag{48}$$

Having demonstrated that we have indeed found localized solutions for all Ω, we shall now derive approximate formulas to describe the main (not the asymptotic) part of the soliton. In the two limiting cases of interest $\Omega\to 0$ (nonrelativistic) and $\Omega\to 1$ (highly relativistic), the right-hand side is dominated by the second and the first terms, respectively. Naturally, in the nonrelativistic limit, the asymptotic shape (48), which is the usual soliton solution of the nonlinear Schrödinger equation, pertains for all $|\xi|$.

The highly relativistic large amplitude wave ($\Omega\to 1$, $A_m\gg 1$) is different and considerably more interesting [6]. Barring the exponentially decaying tail, the main body of the soliton is well approximated by

$$A=A_m\cos(\xi/A_m) \tag{49}$$

and has been termed a "cosine" soliton. The general shape of the large-amplitude soliton is displayed in Fig. 1, where the amplitude A is plotted as a function of ξ. The exact solution is barely distinguishable from (49) in the nonasymptotic region. Equation (49) also predicts that for $A_m>1$, the soliton width L_m is linearly proportional to A_m.

The total plasma density variation associated with the soliton

$$\delta n=\delta n^+ +\delta n^-\approx A^2 \tag{50}$$

is large for $A^2\gg 1$; the solitons with ultrarelativistic amplitudes create large concentrations of plasma density. The stability of the soliton solution of the NSE can be investigated using the well-known stability criterion of Vakhitov and Kolokolov [12]. According to this criterion the soliton is stable if

$$\frac{\partial N}{\delta\Omega^2}>0\ , \tag{51}$$

where N represents the "number of photons"

$$N=\int d\xi\, A^2\ . \tag{52}$$

From a direct integration of the defining equations, one finds

$$N=A_m(1+A_m^2)^{1/2}+\tfrac{1}{2}(1+A_m^2)^{3/2}\arccos\left[\frac{1-A_m^2}{1+A_m^2}\right] \tag{53}$$

and it is trivial to see that $\partial N/\partial\Omega^2=(\partial N/\partial A_m^2)\partial A_m^2/\partial\Omega^2=(1-\Omega^2)^{-2}\partial N/\partial A_m^2>0$, proving the stability of the one-dimensional soliton for all Ω.

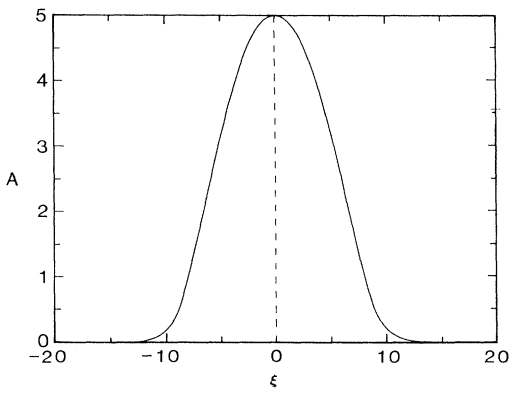

FIG. 1. Typical large amplitude structure A versus ξ. Barring the exponentially decaying tail ($|\xi|>10$), the rest of the soliton is very well approximated by the "cosine" formula.

We conclude that it is possible to obtain a large-amplitude soliton solution in an unmagnetized hot plasma consisting of electrons, positrons, and a small fraction of massive ions. We assert that the presence of even a very small fraction of massive ions is crucial to the soliton formation; a pure electron-positron plasma cannot sustain this disturbance. The e.m. wave pulse with arbitrary amplitude, under certain given conditions, will always spread out in a pure electron-positron plasma [13]. The addition of a small fraction of massive ions stops the pulses from spreading out; the solitons will emerge from the modulational interactions of these pulses. We note in passing that such soliton potentials propagating with $v_g \approx c$ could readily cause acceleration of resonant particles [14].

We now generalize our results by allowing a transverse variation of the fields. If we assume that in Eq. (44) $\Delta_\perp A \gg \partial^2 A/\partial\xi^2$ [note that this condition corresponds to $\omega_0^2 \Delta_\perp A \gg (\partial^2 A/\partial\xi^2)$ in Eq. (43); there was a rescaling of variables from (43) to (44)], then with the ansatz (45) we obtain

$$\frac{\partial^2 A}{\partial r^2}+\frac{1}{r}\frac{\partial A}{\partial r}-\Omega^2 A+A\left[1-\frac{1}{(1+A^2)^2}\right]=0 \quad (54)$$

for the cylindrically symmetric configuration.

We solve this nonlinear eigenvalue problem numerically for the ground state solution [12] $[(dA/dr)_{r=0}=0, A(\infty)=0]$. However, for the ultrarelativistic case, for the region where $A_m \geq A \gg 1$, the solution of Eq. (54) is simply the zeroth-order Bessel function

$$A = A_m J_0(kr) , \quad (55)$$

where $k=(1-\Omega^2)^{1/2}$. In the asymptotic region, the solution must decay and Eq. (54) is solved by the modified Bessel function

$$A \sim K_0(\Omega r) \sim \frac{1}{(\Omega r)^{1/2}} \exp(-\Omega r) , \quad (56)$$

revealing the characteristic exponential decay. The numerical solution of Eq. (54) (solid line) along with the analytical expression (55) (dashed line) is displayed in Fig. 2. In this example the eigenvalue $\Omega^2=0.952\,71$ $[A(0)=A_m=8]$. One can see that the main part of the solution is again very well described by the analytical Bessel function solution (55), the radial analog of the axial cosine soliton [Eq. (49)]. In Fig. 3, we plot the numerically calculated nonlinear dispersion relation $\Omega^2=\Omega^2(A_m)$ (solid line). It is clear that for large-amplitude ($A_m \gg 1$) e.m. waves, $\Omega^2 \to 1$. Let us define the effective width of the soliton as

$$a_{\text{eff}}=\frac{1}{N}\int_0^\infty dr\, r^3 A^2 , \quad (57)$$

where

$$N=\int_0^\infty dr\, r A^2 . \quad (58)$$

In Fig. 4 we plot the numerically obtained relation between the soliton effective width (a_{eff}) and the amplitude A_m (solid line). Note that, as in the axial case, the soliton width is an increasing function of the amplitude $A_m > 1$.

For the large-amplitude case, the "stability integral" N

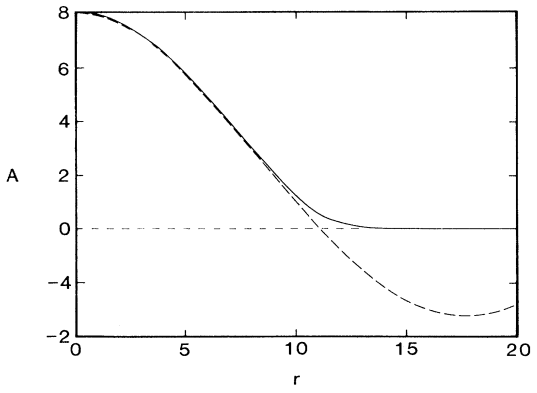

FIG. 2. Comparison of the numerical 2D solution with the Bessel function approximation [Eq. (55)]. There exists excellent agreement for the bulk of the structure.

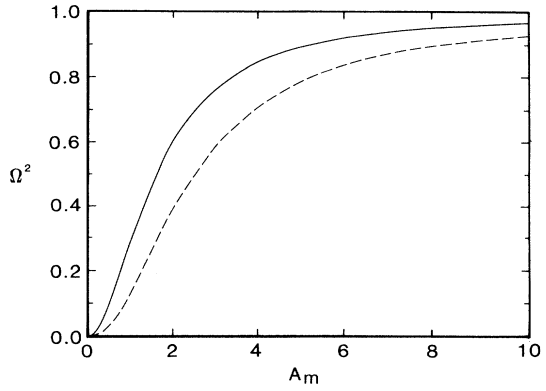

FIG. 3. Nonlinear dispersion relations: the effective eigenvalue Ω^2 as a function of A_m, the amplitude. The solid line corresponds to the 2D case and the dashed line to the 3D case. As $A_m \to \infty$, $\Omega^2 \to 1$.

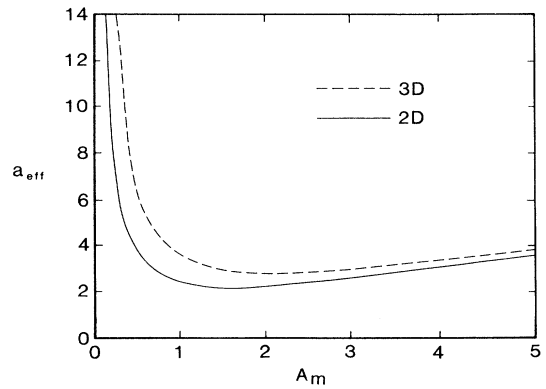

FIG. 4. Effective width a_{eff} versus the amplitude A_m for the 2D (solid line) and the 3D (dashed line) calculations.

will be dominated by contributions from the region in which the Bessel function solution holds. Simple algebra leads us to

$$N=\frac{A_m^2}{k^2}\int_0^C dx\, x\, J_0^2(x)>0\ , \tag{59}$$

where C is a constant of the order unity. From (59) and from the condition $\partial A_m/\partial\Omega^2>0$ (see Fig. 3), we get that $\partial N/\partial\Omega^2>0$. This proof is clearly not formal, but it is quite adequate for the large-amplitude solitons. Using detailed computer simulations, we found that stability criterion $\partial N/\partial\Omega^2>0$ is satisfied for arbitrary amplitude soliton solutions. The dependence of N on Ω^2 is plotted in Fig. 5. Note that if $\Omega^2\to 0$ (i.e., $A_m\to 0$), then $N\to 0.93$, which corresponds to well known "critical power" of the NSE with the cubic nonlinearity $f(|A|^2)=2|A|^2$. Both the cosine and the Bessel function solution were reported in [6].

Now let us consider the stationary solution of Eq. (44) when $\partial^2 A/\partial\xi^2\sim\Delta_\perp A$. It is natural now to look for a "spherical" symmetric distribution of the fields. In terms of the radial variable $r=(x^2+y^2+\xi^2)^{1/2}$, and with the substitution (45), we find

$$\frac{d^2A}{dr^2}+\frac{2}{r}\frac{dA}{dr}-\Omega^2 A+A\left[1-\frac{1}{(1+A^2)^2}\right]=0\ . \tag{60}$$

Like in the cylindrically symmetric configuration, we solve this nonlinear eigenvalue problem numerically for the ground state solution. However, for the ultrarelativistic case it is again possible to get a nearly analytical solution. Indeed for the region where $A_m\geq A\gg 1$, the solution of Eq. (60) is

$$A=A_m\frac{\sin(kr)}{kr} \tag{61}$$

and in the asymptotic region ($r\to 0$) the solution must decay as

$$A\sim\frac{1}{\Omega r}\exp(-\Omega r)\ . \tag{62}$$

The salient features of the solutions presented until now are quite generic to the solution for the NSE with saturating nonlinearities [15]. The numerical solution of

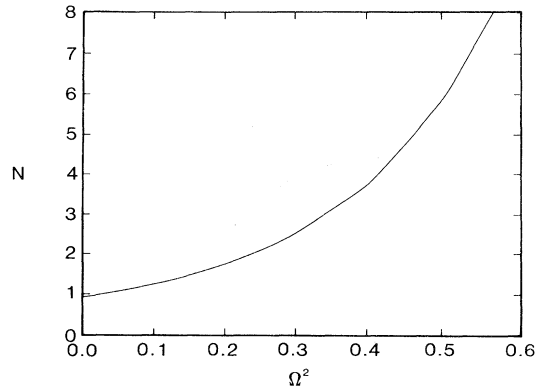

FIG. 5. 2D "stability integral" N versus Ω^2. $N\to 0.93$ as $\Omega^2\to 0$.

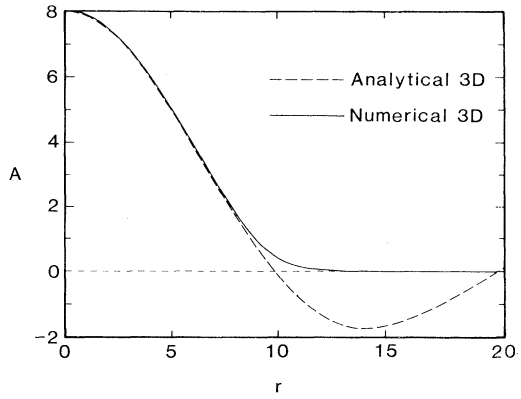

FIG. 6. Comparison of the numerical 3D solution (solid line) with the analytical expression (61) (dashed line). Again there exists good agreement for the bulk of the structure.

Eq. (60) (solid line), along with the analytical expression (61) (dashed line), is displayed in Fig. 6. In this example the eigenvalue $\Omega^2=0.898\,09$ ($A_m=8$). One can see that the main part of the solution is approximated rather well by the analytical expression (61), the spherical analog of the axial cosine, and the cylindrical Bessel solitons. The nonlinear dispersion relation $\Omega^2=\Omega^2(A_m)$ is displayed in Fig. 3 (dashed line). Note that if $A_m\gg 1$, $\Omega^2\to 1$ and for a given amplitude A_m of the e.m. wave, Ω spherical is always less than Ω cylindrical. In Fig. 4 we plot the soliton effective width (a_{eff}) as a function of the amplitude A_m (dashed line).

For the large-amplitude case, the "stability integral" N will be dominated by contributions from the region in which the solution (61) holds. Simple algebra leads us to

$$N=\int_0^\infty dr\, r^2 A^2\approx\frac{A_m^2}{2k^3}C\ . \tag{63}$$

From (63), the condition $\partial A_m/\partial\Omega^2$ (see Fig. 3) implies $\partial N/\partial\Omega^2>0$. Thus, for all cases considered, the large-amplitude soliton solutions of Eq. (44) are stable. The dependence of N on Ω^2, which is found by computer simulation, is presented in Fig. 7. One can see that the

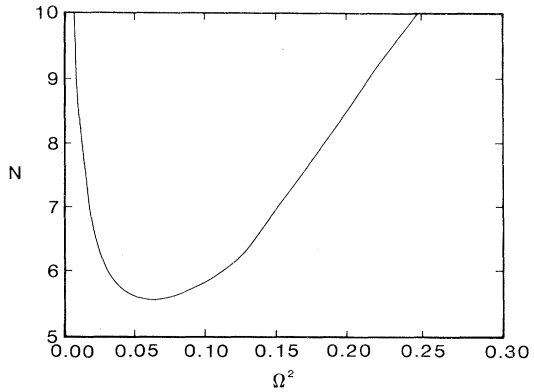

FIG. 7. 3D stability integral versus Ω^2. The stability condition ($\partial N/\partial\Omega^2>0$) holds for Ω^2 greater than a critical value $\Omega^2\approx 0.06$.

stability condition is satisfied for Ω^2 greater than a certain critical value Ω_{cr}^2 ($A_m \approx 0.07$).

Such localized stable objects (using the novel terminology of [16]) can be called "light bullets." Indeed in our case, the solutions represent nondiffracting and nondispersing light pulses with ultrarelativistically strong field amplitudes. Since these pulses carry large density excesses ($\delta n \sim A_m^2 \gg 1$) with them, they could be called heavy bullets of light.

IV. DYNAMIC PROPAGATION

The soliton solutions found in the preceding section represent a class of particular solutions of Eq. (44). It is well known that exact analytical solutions for the NSE with a cubic nonlinearity can be obtained in slab geometry; this equation can be solved exactly using the inverse-scattering technique [17]. For the NSE with a saturating nonlinearity [such as Eq. (44)] the exact analytical methods to derive nonstationary solutions do not exist. One often has to resort to computer simulations to investigate the solutions of such equations. However, general dynamical properties of nonstationary solutions are rather complex, making analytical approximations highly desirable. To describe the dynamics of the localized solutions of the NSE, various approximation schemes, such as the paraxial ray theory [18], the moment theory [19], and the variational approach [20], have been devised.

In the present work we shall follow the variational approach. We will concentrate on the cylindrical symmetric case described by the time-dependent equation

$$i\frac{\partial A}{\partial \tau}+\frac{1}{r}\frac{\partial}{\partial r}r\frac{\partial A}{\partial r}+f(|A|^2)A=0 , \tag{64}$$

where $f(|A|^2)$ is defined by Eq. (42). In a recent paper devoted to the problem of the self-focusing of e.m. waves [21], we have obtained an analytical solution of Eq. (64) by using the paraxial-ray approximation. In this paper we abandon the paraxial-ray approximation because the variational scheme yields much more accurate results. The first step is to construct the Lagrangian

$$L=-r\left|\frac{\partial A}{\partial r}\right|^2+\frac{i}{2}r\left[A^*\frac{\partial A}{\partial \tau}-A\frac{\partial A^*}{\partial \tau}\right]+rF(|A|^2) , \tag{65}$$

where the asterisk denotes a complex conjugate and

$$F(t)=\int_0^t f(t')dt'=\frac{t^2}{1+t} , \tag{66}$$

whose appropriate variation ($\delta L/\delta A^*=0$) within the framework of the variational principle

$$\delta\int\int L\left[A,A^*,\frac{\partial A}{\partial r},\frac{\partial A^*}{\partial r},\frac{\partial A}{\partial \tau},\frac{\partial A^*}{\partial \tau}\right]dr\,d\tau=0 , \tag{67}$$

yields Eq. (64) as the Euler-Lagrange equation.

In the optimization procedure, the first variation of the variational functional must vanish on a set of suitably chosen trial functions. To make the time-dependent problem tractable, an averaging over the radial coordinate is helpful. To do so we have to specify the radial shape of the pulse with time-dependent "shape" parameters. As trial functions, we will use Gaussian shaped pulses, which greatly simplify calculations. Thus we assume that the subsequent evolution of the wave field can be characterized by the trial function

$$A=A_1(\tau)\exp\left[-\frac{1}{2}\frac{r^2}{a^2(\tau)}+ir^2b(\tau)+i\psi(\tau)\right] , \tag{68}$$

which will be used in making the variational functional an extremum. This trial function is parametrized by four real functions: the pulse amplitude $A_1(\tau)$, the pulse width $a(\tau)$, the phase-front curvature $b(\tau)$, and the overall phase $\psi(\tau)$; these functions are allowed to vary with time. Using Eq. (68), the Lagrangian [Eq. (65)] can be expressed in terms of the characteristic parameters of the trial function

$$L=-r^3|A|^2\left[\frac{1}{a^4}+4b^2\right]-r|A|^2\left[\frac{d\psi}{d\tau}+r^2\frac{db}{d\tau}\right]+rF(|A|^2) . \tag{69}$$

Averaging over the radius gives us

$$\langle L\rangle=\int_0^\infty dr\,L=-\frac{A_1^2}{2}\left[1+a^4\left[4b^2+\frac{db}{d\tau}\right]+a^2\frac{d\psi}{d\tau}\right]+\frac{a^2}{2}K(A_1^2) , \tag{70}$$

where

$$K(t)=\int_0^t dt'\frac{F(t')}{t'}=t-\ln(1+t) . \tag{71}$$

The reduced variational principle now can be written as

$$\delta\int_0^\infty d\tau\langle L\rangle(A_1^2,a^2,b,\psi)=0 \tag{72}$$

and the set of Euler-Lagrange equations can be derived by demanding that the variation with respect to each of the unknown functions be zero,

$$\frac{\delta\langle L\rangle}{\delta Q}=0 , \tag{73}$$

where $Q\equiv(A_1^2,a^2,b,\psi)$. After some simple algebra, we get the set of ordinary differential equations

$$\frac{1}{4}\frac{d^2a}{d\tau^2}=\frac{1}{a^3}-\frac{F(A_1^2)-K(A_1^2)}{aA_1^2} , \tag{74}$$

$$\frac{d\psi}{d\tau}=-\frac{2}{a^2}+\frac{2F(A_1^2)-K(A_1^2)}{A_1^2} , \tag{75}$$

$$A_1^2a^2=A_m^2a_0^2 , \tag{76}$$

$$b=\frac{1}{4a}\frac{da}{d\tau} \tag{77}$$

to be solved for the four functions $A_1, a, b,$, and ψ. Equa-

tion (76) is nothing but a statement of the fact that the product of the amplitude and the radial half-width (which is identically equal to the radius) of the pulse is an invariant equal to $A_m a_0$, where A_m and a_0 are, respectively, the initial amplitude and the initial radius. Using (76), the integration of Eq. (74) gives

$$\frac{1}{4}\left[\frac{da}{d\tau}\right]^2 + V(a^2) = E = V(a_0^2) , \tag{78}$$

where E is a constant of integration and

$$V(a^2) = \frac{1}{a^2} - \frac{a^2}{a_0^2 A_m^2} K\left[\frac{A_m^2 a_0^2}{a^2}\right]$$
$$\equiv \frac{1}{a^2} - 1 + \frac{a^2}{a_0^2 A_m^2} \ln\left[1 + \frac{A_m^2 a_0^2}{a^2}\right] \tag{79}$$

plays the role of an effective potential for the "motion" of the radius a. We have also assumed the initial beam to have a plane front ($da/d\tau|_{\tau=0}=0$). Note that in deriving the system of equations (74)–(79), we did not use explicit forms for the functions F and K; thus the analysis can be applied to the NSE with an arbitrary nonlinear term.

Pushing the analogy with a particle (in a potential well) further, we can acquire a deeper physical understanding of the dynamics of the light beam. Let us first explore the possibility of stationary self-trapping of the light beam, the situation when diffraction exactly balances the nonlinearity. Taking the initial radius $a_0 = a_e$, where a_e is the equilibrium radius of the beam, we have a stationary solution if $\partial V/\partial a^2|_{a=a_e}=0$. [Note that $\partial V/\partial a^2$ is equal to the right-hand side of Eq. (74).] The equilibrium radius of the beam is readily found to be

$$\frac{1}{a_e^2} = \frac{1}{A_m^2}[F(A_m^2) - K(A_m^2)]$$
$$= \left[\frac{\ln(1+A_m^2)}{A_m^2} - \frac{1}{1+A_m^2}\right] > 0 , \tag{80}$$

with the nonlinear frequency shift given by

$$\Omega^2 = \frac{d\psi}{d\tau} = \frac{K(A_m^2)}{A_m^2} = 1 - \frac{\ln(1+A_m^2)}{A_m^2} . \tag{81}$$

Let us compare the variational results represented by Eqs. (80) and (81) with the exact results obtained by a direct numerical integration (see Sec. III) of Eq. (64). In Figs. 8 and 9 we display Ω^2 versus A_m and a_e versus A_m plots, respectively, for the numerical calculation (dashed line) and for the relevant analytical formula (solid line). One can see that the results obtained by the variational approach are reasonably close to the exact solutions. We would like to mention that, although the paraxial ray theory does qualitatively describe the dynamics of the e.m. beam, its results show a considerable quantitative difference from the results of the exact numerical and variational approaches. For example, for the equilibrium beam radius, the paraxial theory gives $a_e = (1+A_m^2)^{3/2}/2^{1/2} A_m$ [21], which for $A_m \gtrsim 1$ seriously overestimates the value of the equlibrium radius of the light beam (see Fig. 9, the asterisk-dashed line).

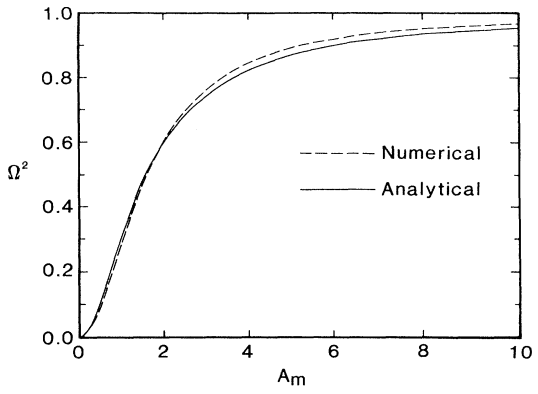

FIG. 8. Comparison of the 2D numerical results (dashed line) with the 2D analytic [Eq. (81), solid line] nonlinear dispersion relation Ω^2 versus A_m.

The stability of the equilibrium solution can be checked by studying the behavior of small-amplitude disturbances around the equilibrium solution $a_0 = a_e$. Linearizing Eq. (74) around the equilibrium solution ($a = a_e + \delta a$, $a_e \gg \delta a$) we get

$$\frac{1}{4}\frac{d^2\delta a}{d\tau^2} + \Omega_e^2 \delta a = 0 , \tag{82}$$

where

$$\Omega_e^2 = \frac{2}{a_e^2}\left[\frac{2}{a_e^2} - \frac{A_m^2}{(1+A_m^2)^2}\right] . \tag{83}$$

Using Eqs. (66) and (80), it can be shown that Ω_e^2 is always positive and consequently the equilibrium solution is stable. Thus the results of variational approach support the exact numerical and analytical results obtained in Sec. III.

Now let us discuss the nonequilibrium solutions of Eq. (78). Note that the effective potential $V(a^2) \to \infty$ as $a \to 0$ and for increasing a, $V(a^2)$ decreases until it

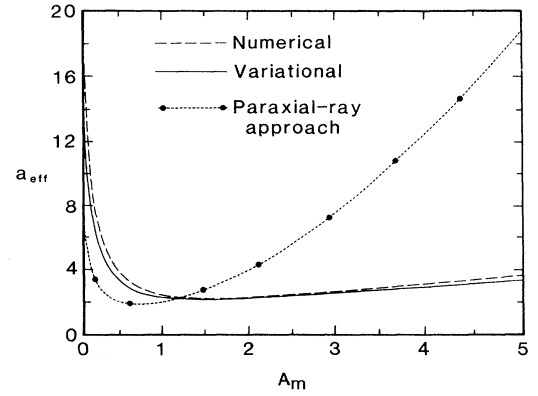

FIG. 9. Comparison of the 2D numerical results (dashed line) with the 2D variational results for the plot a_e versus A_m. The asterisk-dashed line corresponds to results found by the paraxial ray approach.

reaches a minimum and then increases to its asymptotic value $V(\infty)=0$. The qualitative behavior of the time-dependent propagation is clearly controlled by the nature of $V(a)$. If $V(a_0^2)\equiv E<0$, i.e., if [see Eq. (79)]

$$a_0 > a_1 = \left[1-\frac{\ln(1+A_m^2)}{A_m^2}\right]^{-1/2}, \tag{84}$$

then there are two turning points (a_- and a_+) in the potential well. As a result, the beam radius will oscillate between these two values. For the oscillating beam-radius case, there are two distinct modes of behavior: (i) when $a_0 > a_e$ (note that $a_e > a_1$ must always be true), the beam radius initially contracts until it reaches the minimum value given by the turning point $a_- < a_e$; (ii) on the other hand, if $a_e > a_0 > a_1$, the beam radius initially increases (diffraction) until it reaches its maximum value corresponding to the turning point $a_+ > a_e$. In either case, the beam radius is bounded between a_0 and $a_-(a_+)$.

In the opposite limit when $a_0 < a_1$ we have only one turning point ($a=a_0$) and consequently the beam spreads out monotonically. Note that the amplitude of the e.m. beam $A_1(\tau)$ follows the beam radius as $A_1(\tau)=A_m a_0/a(\tau)$. In Fig. 10 we summarize the beam behavior in various distinct regions.

In the preceding analysis, we employed a variational approach involving a Gaussian trial function. It is also possible to use different kinds of trial functions such as the super Gaussian [20], which may fit the equilibrium profile better than the Gaussian. However, for the non-steady propagation, our approach provides explicit, although approximate, analytical expressions for the beam parameters.

We must now emphasize that the main shortcoming of these various integral approaches—the variational and the moments theory—is their inability to account for structural changes in the beam shape (i.e., aberrationless approximation). For example, neither of these schemes can predict that a sufficiently broad beam can undergo "filamentations" as it propagates [22]. Such aspects of the beam dynamics are better delineated by numerical simulation.

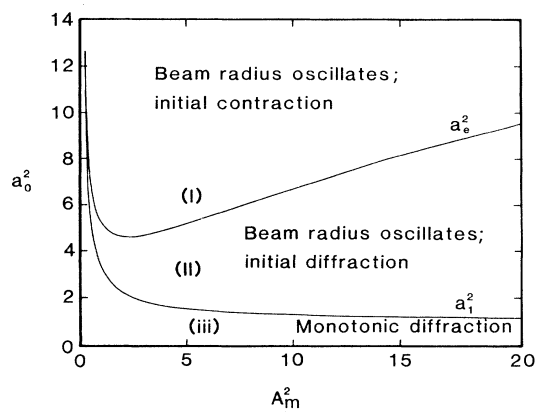

FIG. 10. Classification of regions in the a_0^2-A_m^2 (a_0 is the initial radius and A_m is the initial amplitude of the beam) plane. For $a_0 < a_1$, the beam monotonically diffracts while for $a_0 > a_1$, the beam radius remains bounded but oscillates as the beam propagates. When $a_0 > a_e$ also, then there is initial self-focusing until the beam reaches the lower radius $a_- < a_e$. If a_0 is the range $a_e > a_0 > a_1$, the beam initially diffracts until it acquires its maximum radius $a_+ > a_e$.

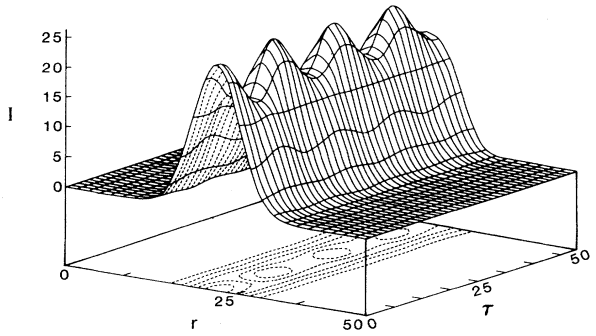

FIG. 11. Field intensity $I=|A|^2$ versus r and τ for initially Gaussian shaped beam $|A(r,0)|=A_m\exp[-(r-r_0)^2/2a_0^2]$ in the case $A_m=5$, $a_0=5$. The beam is trapped in an oscillating waveguide. This curve is the result of direct numerical integration of Eq. (44).

In a recent investigation with Abramyan, we have carried out systematic computer simulations of Eq. (64) and its slab geometry version [23]. It is shown that several aspects of the beam dynamics closely follow the prediction of variational approach, for example, the classification of the beam dynamics based upon the critical radius (Fig. 10). Here we present several figures from [23]. In Fig. 11 we plot the field intensity ($I=|A|^2$) distribution versus r and τ for the initially Gaussian shaped beam $|A(r,0)|=A_m\exp[-(r-r_0)^2/2a_0^2]$, where the beam width $a_0=5$ and the beam amplitude is relativistically strong $A_m=5$. This case corresponds to beam self-trapping in an oscillating waveguide. In Fig. 12 we present the case when the beam amplitude is the same, but its width $a_0=20$ is much greater. One can see that for this large width, the beam filaments as it propagates.

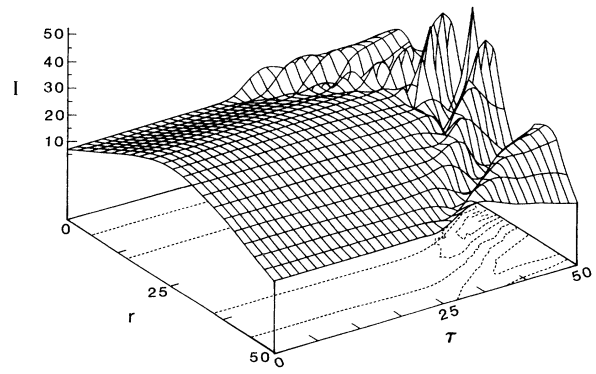

FIG. 12. Field intensity I versus r and τ in the case of $A_m=5$, $a_0=20$. The filamentation of the beam profile takes place as the beam propagates. This kind of behavior cannot be captured by approximate "integral" methods such as the variational or the moment approach.

Note that in this case the beam width (a_0) is approximately five times larger than the equilibrium width a_e corresponding to $A_m = 5$. In the jargon used in "laser interactions with nonlinear media," this situation corresponds to the case when the beam power ($\sim a_0^2 A_m^2$) is much larger than the critical power ($\sim a_e^2 A_m^2$) and as a result the beam breaks down into a set of narrow channels ("filaments"), each with a power content of the order of the critical power.

In this section we have limited ourselves to the study of the e.m. beams with cylindrical profiles. [Note that one spatial coordinate may be replaced by a "moving" coordinate ($\xi = z - v_g t$), thus creating a light bullet.] For the case of Cartesian or spherically symmetric beams it is also possible to develop a variational approach. We do not discuss these results here because algebraic complications make them less transparent. However, solutions of Eq. (44) in a general geometry will be interesting for nonlinear optics and will be presented elsewhere.

Finally, we would like to remind the readers about an important general result found by Zakharov, Sobolev, and Synakh [24] using the moment method. It is easy to prove by direct calculation (or by Noether's theorem using the Lagrangian) that Eq. (44) has the integrals of motion

$$N = \int d\mathbf{r} |A|^2 \tag{85}$$

and

$$H = \int d\mathbf{r} \left[|\nabla A|^2 - \frac{|A|^4}{1+|A|^2} \right] , \tag{86}$$

where N is the photon number (i.e., our stability integral for the stationary case) and H can be viewed as an energy integral. For $H < 0$, simple manipulations of Eqs. (85) and (86) can lead to the bound

$$\max |A|^2 > \frac{|H|}{N} . \tag{87}$$

This result is very significant and simply means that if initial field distribution is such that it provides a negative value of H, then the field intensity has a time-independent upper bound. This is precisely the meaning of the term "self-trapping of the beam." It is interesting to note that in regions (i) and (ii) of Fig. 10, where we have self-trapping of the beam, the energy integral is indeed negative. The condition $H < 0$, of course, does not provide us with any details of the time evolution of the light pulse, but is quite general and for any symmetric case gives us the range where we should expect the formation of the localized self-trapped field configurations. The derivation and verification of such general results are two of the main purposes of this paper.

V. CONCLUSIONS

We have investigated the nonlinear propagation of CP e.m. waves in hot unmagnetized *e-p* plasmas with a small fraction of ions. In our analysis, we included not only the ponderomotive nonlinearity and relativistic effects in the hydrodynamic motion of the plasma, but also the effects that result from the relativistic electron velocity distribution. We concentrated on the case of a transparent plasma and derived the NSE with a saturating nonlinearity. It turns out that in this equation, the role of the particle mass is played by a temperature-dependent "effective mass." We were able to obtain analytical and nearly analytical soliton solutions of this equation. Using analytical and numerical methods we demonstrated the stability of the soliton solutions. These solitons, corresponding to relativistically strong amplitude e.m. waves, carry a large density inhomogeneity, and are nondiffracting and nondispersing localized structures that could be called heavy bullets of light. To understand the main properties of the nonsteady propagation of e.m. pulses, we used a variational approach and found that the main results of the variational approach are confirmed by numerical simulations.

In conclusion, we have shown that in an electron-positron plasma with a small fraction of ions, it is possible to have localized stable structures with large density bunching and with velocities close to the velocity of light—the heavy bullets of light. Such objects could play an important role in cosmology as a source of structure formation in the MeV epoch of the evolution of the Universe. Coupled with gravity, these objects may lead to the creation of large scale inhomogeneity in the Universe. Another potentially important applications of the *e-p-i* plasma may be found in providing an understanding of the nature of the intergalactic jets. Astrophysical objects, such as the radio galaxies, quasars, or radio pulsars could radiate ultrarelativistically strong e.m. pulses, which, in the ever present *e-p-i* plasmas in their vicinity (for example, in the form of relativistic jets), could propagate in self-created channels.

The full impact of our theory on cosmology and on astrophysics cannot be expounded in the present paper. In future work we plan to investigate the problem in more detail.

[1] C. F. Kennel and R. Pellat, J. Plasma Phys. **15**, 335 (1976); J. N. Leboeuf, M. Ashour-Abdalla, T. Tajima, C. F. Kennel, F. Coroniti, and J. M. Dawson, Phys. Rev. A **25**, 1023 (1982); M. E. Gedalin, J. G. Lominadze, L. Stenflo, and V. N. Tsitovich, Astrophys. Space Sci. **108**, 393 (1985); P. K. Shukla, N. N. Rao, M. Y. Yu, and N. L. Tsintsadze, Phys. Rep. **135**, 1 (1986); R. E. Kates and D. P. Kaup, J. Plasma Phys. **41**, 507 (1989).

[2] F. C. Michel, Rev. Mod. Phys. **54**, 1 (1982); M. C. Begelman, R. D. Blandford, and M. D. Rees, *ibid.* **56**, 255 (1984).

[3] S. Weinberg, *Gravitation and Cosmology* (Wiley, New York, 1972); Ya. B. Zeldovich and I. Novikov, *Relativistic Astrophysics* (University of Chicago Press, Chicago, 1983).

[4] J. G. Lominadze, G. Z. Machabeli, G. I. Melikidze, and A. D. Pataraya, Fiz. Plasmy **12**, 1233 (1986) [Sov. J. Plasma Phys. **12**, 712 (1986)]; G. S. Lakhina and B. Buti, Astrophys. Space Sci. **79**, 25 (1981); F. B. Rizzato, J. Plasma Phys. **40**, 289 (1988); V. I. Berezhiani, M. Y. El-Ashry, and U. A. Mofiz, Phys. Rev. E **50**, 448 (1994).

[5] M. Hoshino, J. Arons, Y. Gallant, and A. B. Langdon, Astrophys. J. **390**, 454 (1992).

[6] V. I. Berezhiani and S. M. Mahajan, Phys. Rev. Lett. **73**, 1110 (1994).

[7] J. P. Ostriker, C. Thompson, and E. Witten, Phys. Lett. B **180**, 231 (1986); K. Holcomb and T. Tajima, Phys. Rev. D **40**, 3909 (1989); T. Tajima and T. Taniuti, Phys. Rev. A **42**, 3587 (1990).

[8] L. D. Landau and E. M. Lifshitz, *Hydrodynamics* (Science, Moscow, 1986); D. I. Dzhavakhishvili and N. L. Tsintsadze, Zh. Eksp. Teor. Fiz. **64**, 1314 (1973) [Sov. Phys. JETP **37**, 666 (1973)]; S. V. Kuznetsov, Fiz. Plasmy **8**, 352 (1982) [Sov. J. Plasma Phys. **8**, 199 (1982)].

[9] L. D. Landau and E. M. Lifshitz, *Classical Theory of Field* (Pergamon, Oxford, 1975).

[10] V. I. Berezhiani, V. Skarka, and S. M. Mahajan, Phys. Rev. E **48**, R3252 (1993).

[11] X. L. Chen and R. N. Sudan, Phys. Fluids B **5**, 1336 (1993).

[12] J. Juul Rasmussen and K. Rypdal, Phys. Scr. **33**, 481 (1986), see Ref. 96 therein; E. A. Kuznetsov, V. E. Rubenchik, and V. E. Zakharov, Phys. Rep. **142**, 103 (1986).

[13] V. I. Berezhiani, L. N. Tsintsadze, and P. K. Shukla, J. Plasma Phys. **48**, 139 (1992).

[14] P. K. Kaw, A. Sen, and T. Katsouleas, Phys. Rev. Lett. **68**, 3172 (1992).

[15] K. Hayata and M. Koshiba, J. Appl. Phys. **71**, 2526 (1991).

[16] Y. Silberberg, Opt. Lett. **15**, 1282 (1990).

[17] V. E. Zakharov and A. B. Shabat, Zh. Eksp. Teor. Fiz. **61**, 118 (1971) [Sov. Phys. JETP **34**, 62 (1972)].

[18] S. A. Akhmanov, A. P. Sukharukov, and R. V. Khokhlov, Usp. Fiz. Nauk **93**, 19 (1967) [Sov. Phys. Usp. **10**, 609 (1968)].

[19] J. F. Lam, B. Lippman, and F. Tappert, Phys. Fluids **20**, 1176 (1977).

[20] D. Anderson and M. Bonnedal, Phys. Fluids **22**, 105 (1979); D. Anderson, M. Bonnedal, and M. Lisak, Phys. Fluids **22**, 1838 (1979); D. Anderson, Phys. Rev. A **27**, 3135 (1983); M. Karlsson, *ibid.* **46**, 2726 (1992).

[21] V. I. Berezhiani and S. M. Mahajan, Astrophys. Space Sci. **222(1/2)**, 241 (1994).

[22] F. S. Felber, Appl. Phys. Lett. **8**, 18 (1981).

[23] L. A. Abramyan, V. I. Berezhiani, and S. M. Mahajan (unpublished).

[24] V. E. Zakharov, V. V. Sobolev, and V. C. Synakh, Zh. Eksp. Teor. Fiz. **60**, 136 (1971) [Sov. Phys. JETP **33**, 77 (1971)].